Mechanism of hydrazine oxidation at Palladium electrodes: Long-lived radical di-cation formation

Ruiyang Miao, Richard G Compton*

Department of Chemistry, Physical and Theoretical Chemistry Laboratory,

University of Oxford, South Parks Road,

Oxford OX1 3QZ, Great Britain

*Corresponding author

Email: richard.compton@chem.ox.ac.uk

Phone: +44 (0) 1865 275957 Fax: +44 (0) 1865 275410

Highlights

- Both N_2H_4 and $N_2H_5^+$ are electro-active at Palladium electrodes.
- A hitherto unsuspected long-lived radical di-cation $N_2H_5^{\bullet 2+}$ is an intermediate
- The radical di-cation is formed during the electrolysis of $N_2H_5^+$ but not N_2H_4.

Table of Contents

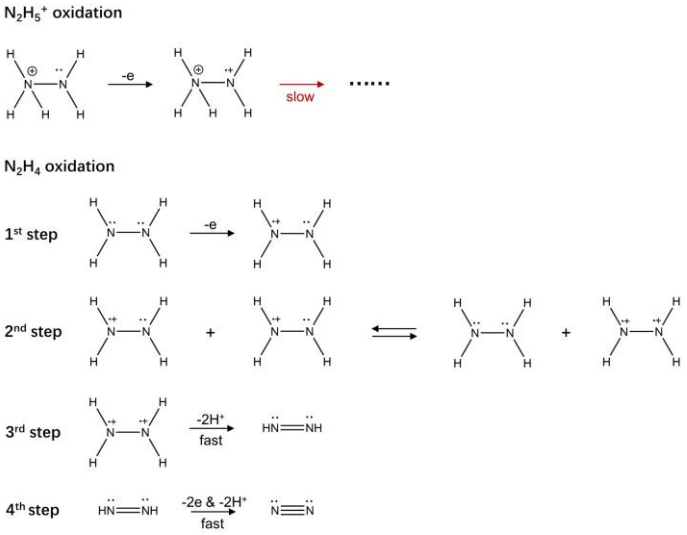

The electro-oxidation of hydrazine over the pH range 2 to 11 is studied mechanistically and a hitherto unsuspected radical di-cation resulting from the one electron oxidation of the hydrazinium cations, $N_2H_5^+$, is observed voltammetrically

Abstract

The mechanism of the catalytic oxidation of hydrazine at Palladium (Pd) electrodes was studied in aqueous solutions between pH 2 and 11. The voltammetry recorded at pH 2 and 11 revealed that both the unprotonated hydrazine N_2H_4 and the protonated form $N_2H_5^+$ are electro-active at the Pd surface in contrast to glassy carbon (GC) where N_2H_4 is the only species which undergoes oxidation in the potential range of 0.2 to 1.0 V (vs the Saturated Calomel Electrode).

An unexpected reductive voltammetric wave was observed during the cyclic voltammetry of the oxidation of protonated hydrazine and concluded to originate from the reduction of a radical di-cation $N_2H_5^{\bullet 2+}$ which is stable on the voltammetric timescale. The di-cation was inferred to result from the loss of one electron from the single lone pair of electrons on $N_2H_5^+$. It is suggested that, unlike the case of N_2H_4, the absence of a lone pair on the N adjacent to that being oxidised as a result of protonation leads to the stability of the radical di-cation whereas in the oxidation of N_2H_4, the available adjacent lone pair facilitates rapid follow up chemical reaction leading to nitrogen formation.

Keywords: hydrazine oxidation; electron transfer; radical di-cation; electro-catalysis; Palladium

1. Introduction

The four electron electro-oxidation of hydrazine to nitrogen in aqueous solution, under alkaline conditions,

$$N_2H_4(aq) - 4e = N_2(g) + 4H^+(aq),$$

and under acidic conditions,

$$N_2H_5^+(aq) - 4e = N_2(g) + 5H^+(aq)$$

is of both applied and fundamental significance in respect of fuel cells [1-4] and sensors [5-8], with recent insightful contributions from Ulstrup and colleagues [1, 8]. Extensive efforts have been placed on the development of high-performance electro-catalysts towards hydrazine oxidation, especially including noble metal and their use in decoration. For example, Wu et al. [9] reported that the catalyst palladium decorated porous nickel synthesized via de-alloying and galvanic replacement, displayed outstanding electro-catalytic properties towards hydrazine oxidation as well as good long-term durability with only 5% loss of its initial current density after 1000 cycles. Ghasemi et al. [10] fabricated an amperometric nanosensor with platinum-palladium nanoparticles decorated reduced graphene oxides, and it exhibited an excellent sensing performance with a linear response range between 0.007 - 5.5 mM and a 1.7 μM detection limit. Notwithstanding the great progress made empirically, the understanding of the mechanism of the four electron, four/five proton hydrazine oxidation remains challenging, but vital to provide generic guidance for catalyst design.

We have recently explored the hydrazine oxidation at glassy carbon electrodes [11, 12] in aqueous solutions where the following equilibrium is important

$$N_2H_5^+ \rightleftharpoons N_2H_4 + H^+$$

Our previous study [12] demonstrated that $N_2H_5^+$ does not undergo oxidation on the surface of glassy carbon over a wide range of potentials whereas the oxidation of N_2H_4 proceeds cleanly albeit with significant over-potential. Importantly from a mechanistic perspective the protons generated from the N_2H_4 oxidation easily combine with the N_2H_4 molecules diffusing to the electrode surface, to form the inactive $N_2H_5^+$ so to inhibit the oxidation; the reaction is self-inhibiting. This highlights the importance of understanding the chemistry occurring at the catalyst surface as well as the intrinsic electron transfer details. Accordingly, herein we study the electron transfer behaviour of N_2H_4 and $N_2H_5^+$ at the noble metal Pd electrodes in aqueous solutions from pH 2 to 11. It was found that both species are fully *electro-active* at Pd, and notably, a *long-lived* radical di-cation $N_2H_5^{\bullet 2+}$ is generated from the oxidation of $N_2H_5^+$ and has a finite lifetime on the voltammetric timescale (*ca.* seconds). Its existence is likely attributed to the fact that the lone pair on the N adjacent to that being oxidised is pronated and so not available for immediate further reaction in contrast to the oxidation of N_2H_4.

2. Experimental

Chemicals

Hydrazine hydrate ($N_2H_4 \cdot xH_2O$, 98%), potassium monohydrogen phosphate (K_2HPO_4, 98%), potassium dihydrogen phosphate (KH_2PO_4, 99%) and nitric acid (HNO_3, 70%) were purchased from Sigma-Aldrich, Dorset, UK. Potassium hydroxide (KOH, 85%) and potassium nitrate (KNO_3, 99.99%) were obtained from Fisher Scientific, Loughborough, UK. Nitrogen (N_2, 99.998%) was supplied by BOC, Surrey, UK. All of

the chemicals were used as received without further purification. An aqueous solution of 1.5 mM hydrazine supported by 0.1 M KNO_3 was prepared, of which the pH was measured to be 9.7. Comparable hydrazine solutions of pH 2.0, 5.0, 6.0 and 7.0 were made by additions of tiny amounts of HNO_3 for pH adjustment. A phosphate buffer solution (PBS, 0.1 M, pH 11.0) with 1.5 mM hydrazine was prepared via mixing K_2HPO_4, KH_2PO_4 and hydrazine in water [13]. The water used for the preparation of all solutions was 'ultrapure' with a resistivity of 18.2 MΩ cm at 25 ℃ (Milli-Q lab water system). All pH measurements were made with a digital pH meter (sensION^{TM}+ pH 31) purchased from HACH, Colorado, USA.

Electrochemical measurements

The electrochemical cell consisted of three electrodes: palladium (Pd, diameter in 3.01 mm) or glassy carbon (GC, diameter in 2.95 mm) macrodisc working electrodes, a saturated calomel reference electrode (SCE) and a graphite rod counter electrode. All voltammetric measurements were performed inside a Faraday cage thermostated at 25 ℃, with a μAutolab II potentiostat (Metrohm, Utrecht, NL) using the control software Nova. The surfaces of the Pd and GC electrodes were mechanically polished with alumina slurries of decreasing particle sizes (1.0, 0.3 and 0.05 μm), and rinsed with deionised water before use. Then cyclic voltammetry (CV) measurements were conducted in the abovementioned solutions that were vigorously degassed with N_2 for 15 min so to remove the dissolved oxygen prior to the measurements. The control experiments were undertaken in equivalent media but without hydrazine.

3. Results and discussion

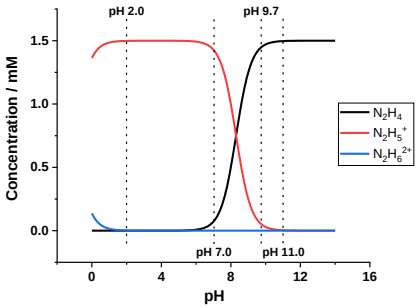

Fig. 1. The speciation of hydrazine calculated as a function of pH in pure water. Black/Red/Blue lines correspond to the concentrations of N_2H_4, $N_2H_5^+$ and $N_2H_6^{2+}$ respectively.

In aqueous solution hydrazine, N_2H_4, acts as a base, the conjugate acid of which has a pK_a value of *ca.* 8.1 at 25 °C [14-17]. Thus at low pH the molecule exists in its protonated form, $N_2H_5^+$, the hydrazinium cation. At extremely low pH this is further protonated to form $N_2H_6^{2+}$ with a pK_a of *ca.* -1.0 [18-20]. Fig. 1 shows how the speciation of a solution of hydrazine varies with pH. In particular at pH 2 the composition is almost entirely $N_2H_5^+$ whereas at pH 11.0 it is overwhelmingly N_2H_4. At pH values of 7 and 9.7 both N_2H_4 and $N_2H_5^+$ co-exist.

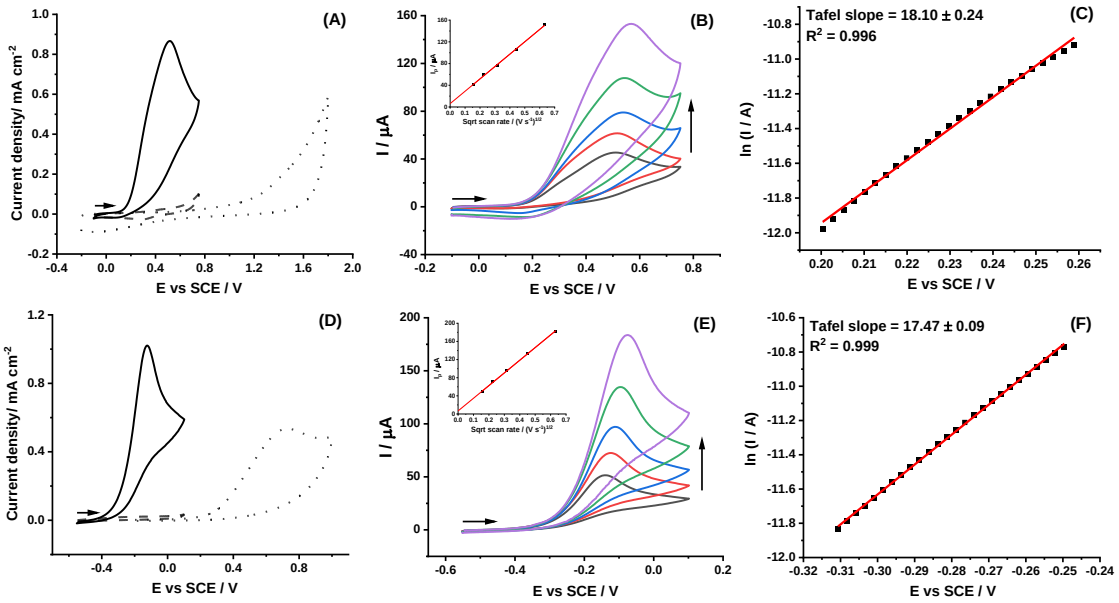

Fig. 2. (A) and (D) Voltammograms measured at 50 mV/s in 0.1 M KNO_3 of pH 2 and 0.1 M PBS of pH 11 respectively: with 1.5 mM hydrazine at a Pd electrode (solid line), without hydrazine at a Pd electrode (dash line) and with 1.5 mM hydrazine at a GC electrode (dot line). (B) and (E) Scan rate study (25/50/100/200/400 mV/s) in 0.1 M KNO_3 of pH 2 and 0.1 M PBS of pH 11 respectively

with 1.5 mM hydrazine at a Pd electrode. The insets are the plots of peak current I_p versus square root of scan rate. (C) and (F) Tafel analysis in the region of 10% to 30% of the oxidative peaks in 0.1 M KNO_3 of pH 2 and 0.1 M PBS of pH 11 respectively with 1.5 mM hydrazine at a Pd electrode. The transverse arrows indicate the start potentials and directions of the voltametric scans. The vertical arrows indicate increasing scan rates.

The comparative electro-catalysis towards hydrazine oxidation was first investigated at Palladium (Pd) and Glassy Carbon (GC) macrodisc electrodes in 1.5 mM hydrazine supported by 0.1 M KNO_3 of pH 2. The pH was controlled by the addition of tiny amounts of HNO_3. As discussed above, under these conditions, protonated hydrazine $N_2H_5^+$ accounts for almost 100% of the hydrazine speciation. The recorded cyclic voltammograms are shown in Fig. 2A. Considering the Pd electrode, a fully electrochemically and chemically irreversible oxidative wave (solid line) is observed at a peak potential of *ca.* 0.52 V vs SCE with a current density of 0.87 mA cm^{-2} at 50 mV/s in the presence of hydrazine whereas no voltammetric features (dash line) are observed in the absence of hydrazine, indicating the significant anodic current results from the oxidation of $N_2H_5^+$ which is well documented to form exclusively N_2 and protons [21, 22]. The dotted curve recorded at the GC electrode clearly shows no oxidative signals of hydrazine, in agreement with our previous work [12] that concluded that $N_2H_5^+$ is fully electro-*inactive* at all potentials in the range studied at a GC electrode. This demonstrates the *effective* catalysis of Pd towards the oxidation of $N_2H_5^+$. The scan rate study at the Pd electrode is depicted in Fig. 2B where the peak current after baseline correction (but without correction for ohmic drop) is seen to be linearly proportional to the square root of scan rate, signalling it is a diffusion-controlled process [23]. Tafel analysis was conducted to extract the Butler-Volmer anodic transfer coefficient β for $N_2H_5^+$ oxidation from the voltammogram (solid line in Fig. 2A). The region from 10%

to 30% of the oxidative peak current was taken for analysis where the mass transport effects can be ignored [24]. The result after baseline correction is displayed in Fig. 2C that gives a transfer coefficient $\beta_{N_2H_5^+}$ value of 0.46 ± 0.01 from the Tafel slope for the oxidation of the hydrazinium cation indicating that removal of the first electron is the rate determining step of the oxidation.

Analogous experiments to those above were performed at both Pd and GC electrodes in 0.1 M PBS of pH 11, where nearly all the hydrazine present exists in the unprotonated form N_2H_4. Fig. 2D shows a fully chemically and electrochemically irreversible voltammetric wave (solid line) at a peak potential of *ca.* -0.12 V vs SCE with a current density of 1.02 mA cm^{-2} for the oxidation of N_2H_4 at the Pd electrode at a scan rate of 50 mV/s. Note that the blank, containing no hydrazine, experiment (dash line) shows no corresponding features. At the GC electrode, an electrochemically irreversible wave with a current density of 0.53 mA cm^{-2} was observed at a peak potential of *ca.* 0.73 V vs SCE indicating the oxidation of N_2H_4 to nitrogen [11, 25]. Comparison of the voltammograms for the oxidation of N_2H_4 at Pd and GC (Fig. 2D) shows that significantly higher overpotential is required at the GC surface than Pd, evidencing Pd to be an *effective* electro-catalyst towards N_2H_4 oxidation. The oxidation is again diffusional as inferred from the peak current (after baseline correction) versus scan rate plot shown in Fig. 2E and a value of the transfer coefficient $\beta_{N_2H_4}$ (0.45 ± 0.01) was obtained via the Tafel analysis in Fig. 2F.

Having evidenced the catalytic ability of Pd towards the oxidation of both N_2H_4 and $N_2H_5^+$, voltammetry was then conducted without the addition of acids or bases. In

particular we studied 0.1 M KNO_3 with 1.5 mM added hydrazine. This solution had a measured pH 9.7 reflecting the equilibrium

$$N_2H_4 + H_2O \rightleftharpoons N_2H_5^+ + OH^-$$

The measured pH was used to estimate the pK_a of hydrazine in 0.1m KNO_3 giving a value of 8.3 ± 0.1 which is close to that cited above but there applying to pure water. The discrepancy can be attributed to a small thermodynamic salt effect [26-28].

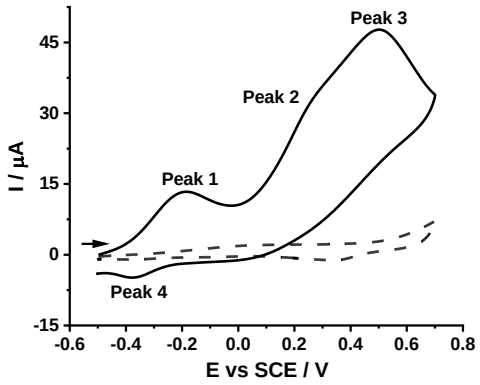

Fig. 3. Voltammogram (solid line) recorded in 0.1 M KNO_3 with 1.5 mM hydrazine (no buffering, measured pH 9.7) at a Pd electrode at 50 mV/s. Also shown is the voltammogram (dash line) under the same conditions but without hydrazine. The transverse arrow indicates the start potential and direction of the voltametric scans.

The voltammetry (solid line) was recorded as illustrated in Fig. 3, of which three oxidative peaks, and most unexpectedly a hitherto unsuspected reductive peak, are clearly seen (labelled in order of the voltammetric scan) in the presence of hydrazine, while there are no voltammetric features seen without hydrazine present (dash line). The peak potentials of Peaks 1, 2, 3 and 4 are *ca.* -0.17, 0.26, 0.50 and -0.37 V vs SCE respectively at the scan rate of 50 mV/s.

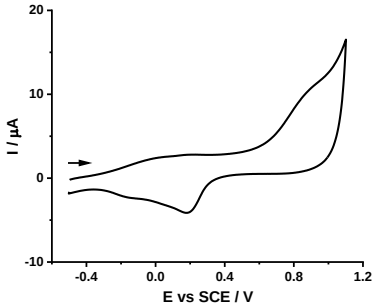

Fig. 4. Voltammograms recorded in 0.1 M KNO_3 (no buffering, pH 9.7) at a Pd electrode at 50 mV/s. The transverse arrow indicates the start potential and direction of the voltametric scan.

It has been reported [29, 30] in the case of the oxidation of hydrazine at platinum electrodes that surface oxides are crucial to the electrocatalysis. So to explore this possibility voltammetry was conducted in the absence of hydrazine at the Pd electrode. As illustrated in Fig. 4, a quasi-irreversible oxidative peak is seen at a peak potential of *ca.* 0.88 V vs SCE. It is clear that the formation of Palladium oxides (PdO) requires a much higher overpotential than hydrazine oxidation (solid line in Fig. 2A) under these conditions. It follows that Peaks 1, 2, 3 and 4 on Fig. 3 are not related to the formation or stripping of PdO, the involvement of which in the hydrazine oxidation were thus discounted, in contrast to the case of Platinum electrodes. The details on the formation of PdO at pH 2, 7 and 11 are presented in the Supporting Information (SI) Section 1. Again no involvement of palladium oxides in hydrazine oxidation at these pH values.

Returning to Fig. 3, it is noticeable that Peaks 1 and 3 show complete consistency in peak potential with the oxidative peaks of N_2H_4 (solid line in Fig. 2A) and $N_2H_5^+$ (solid line in Fig. 2D) respectively. Hence, it is inferred that Peak 1 corresponds to the *direct* oxidation of N_2H_4 while Peak 3 is assigned to the *direct* oxidation of $N_2H_5^+$ as follows:

Peak 1: $N_2H_4 \xrightarrow{-4e} N_2 + 4H^+$

Peak 3: $N_2H_5^+ \xrightarrow{-4e} N_2 + 5H^+$

It is well-known that the chemical equilibrium between the two hydrazine species, protonated or unprotonated, acts in parallel with the electron transfer reactions [31-33]. Importantly the protons from hydrazine oxidation can significantly change the local pH thus in turn affecting the oxidation process [12]. Hence, we infer that Peak 2 likely corresponds to the dissociation of $N_2H_5^+$ to N_2H_4 firstly and the following oxidation of the produced N_2H_4 as follows, distinguished from the direct oxidation of N_2H_4 for Peak 1:

Peak 2: $N_2H_5^+ \rightleftharpoons N_2H_4 + H^+$; $N_2H_4 \xrightarrow{-4e} N_2 + 4H^+$

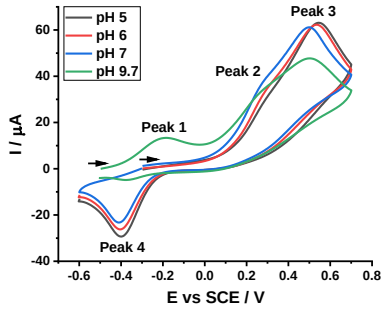

Fig. 5. Voltammograms recorded in 0.1 M KNO_3 with 1.5 mM hydrazine of different pHs (pH 5/6/7/9.7) at a Pd electrode at 50 mV/s. The transverse arrows indicate the start potentials and directions of the voltammetric scans.

A pH study upon hydrazine oxidation was then performed so to further clarify the peak information. The electrolytes in support of 1.5 mM hydrazine were unbuffered, 0.1 M KNO_3, of which the pHs were controlled by additions of tiny amounts of nitric acid so as to realise bulk pH values of 5, 6, 7 and 9.7. The results are shown in Fig. 5. It is clear that an increase in pH leads to the increased anodic current of Peak 1 whereas that of Peak 3 is seen to decrease, in accord with the pH-dependent speciation of N_2H_4 and $N_2H_5^+$ in solutions in Fig. 1. This is consistent with the above inference that Peaks 1 and 3 correspond to the direct oxidation of N_2H_4 and $N_2H_5^+$ respectively, and also accounts for the fact that only one peak is seen at pH 2 or pH 11 since for each there is

the only active hydrazine species, $N_2H_5^+$ or N_2H_4. Meanwhile, an increasing visibility of Peak 2 is qualitatively expected as the pH rises facilitating the dissociation process, and the observed behaviour further qualitatively evidences the involvement of the chemically preceding dissociation reaction in the formation of Peak 2. Moreover, the peak separation between Peaks 1 and 2 induced by the preceding chemical reaction is measured to be *ca.* 0.38 to 0.49 V, where the uncertainty reflects the fact that Peak 2 appears as a shoulder on Peak 3, thus generating an *effective* dissociation constant $K_{a,eff}$ value of approximately 3.3×10^{-4} M to 2.0×10^{-3} M where $K_{a,eff}$ is the product of the true K_a divided by the local proton concentration $K_{a,eff} = K_a / \left[H^+ \right]_{local}$. The latter varies at different potentials on the oxidative wave but a value of *ca.* 10^{-3} M for the local proton concentration in the vicinity of the peak can be inferred suggesting that the estimated value is not inconsistent with the reported value of K_a (8.5×10^{-7} M) [34, 35]. This value quantitatively reflects the role of the chemical equilibrium and local pH change in the oxidation of N_2H_4 and the suggested origin of Peak 2.

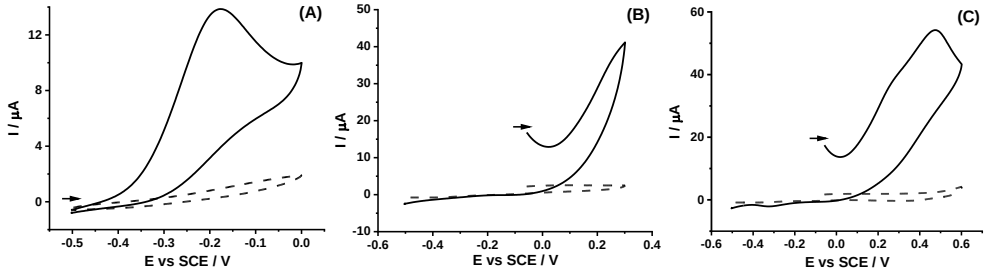

Fig. 6. Voltammograms (solid line) recorded in 0.1 M KNO_3 with 1.5 mM hydrazine (no buffering, measured pH 9.7) at a Pd electrode at 50 mV/s within different potential windows: (A) scan from -0.5 V anodically to 0 then cathodically to -0.5 V, (B) scan from -0.05 V anodically to 0.3 V then cathodically to -0.5 V and (C) scan from -0.05 V anodically to 0.6 V then cathodically to -0.5 V. Also shown are voltammograms (dash line) under the same conditions but without hydrazine. The transverse arrows indicate the start potentials and directions of the voltametric scans.

Next the focus was turned to the investigation of the novel Peak 4 in Fig. 3. A series of variable potential window experiments were carried out to probe into the origin of Peak

4. The voltammetric curve in Fig. 6A was scanned from a start potential of -0.5 V to 0 V at which point it was reversed to -0.5 V. The scan shows *only* an oxidative peak with a current of 13.8 μA at a peak potential of -0.17 V vs SCE (50 mV/s), fully consistent with Peak 1 (Fig. 3). The absence of a back peak indicates no causal connection between Peaks 1 and 4 (Fig. 3). Fig. 6B displays a voltammogram that starts at -0.05 V then scans anodically to 0.3 V and ends at -0.5 V so as to explore any causal relation between peak 4 with peak 2. Again no back peak was observed leading to the conclusion that the reductant for Peak 4 does not originate from the products of Peak 2 which as discussed above relates to the oxidation of N_2H_4 formed by dissociation of $N_2H_5^+$. Then in a third experiment the potential upper vertex was extended to 0.6 V to encompass the direct oxidation of $N_2H_5^+$ (Peak 3) and voltammetry was recorded as presented in Fig. 6C. Two obvious oxidative peak are observed at peak potentials of *ca.* 0.26 V and 0.48 V matching with Peaks 2 and 3 (Fig. 3) respectively. Notably a reductive peak appears at *ca.* -0.33 V which is comparable with Peak 4 in Fig. 3. Therefore, the reductant for Peak 4 is the product from the direct oxidation of $N_2H_5^+$ (Peak 3). The details of the full scan rate study at pH 9.7 within the variable potential windows are given in Fig. 7. All these data point to the origin of Peak 4 resulting from the direct oxidation of $N_2H_5^+$.

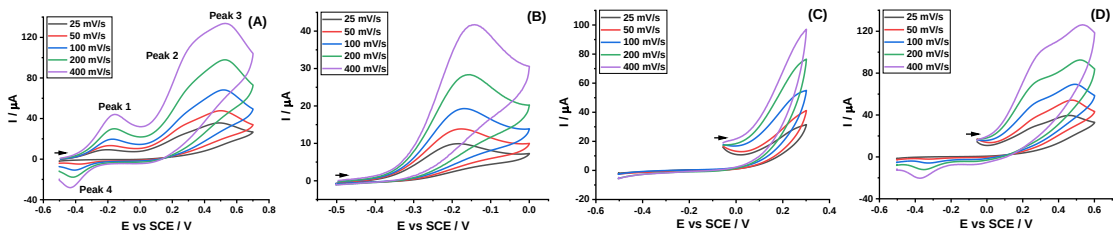

Fig. 7. Voltammograms recorded in 0.1 M KNO_3 with 1.5 mM hydrazine (no buffering, pH 9.7) at a Pd electrode at various scan rates (25/50/100/200/400 mV/s) within different variable potential windows. The transverse arrow indicates the start potential and direction of the voltametric scans.

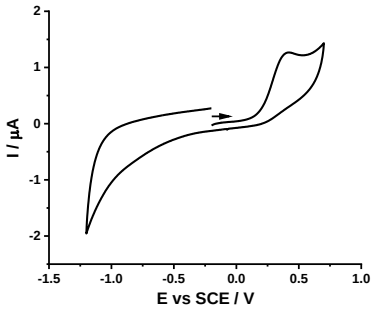

Fig. 8. Voltammogram recoded in 0.1 M KNO_3 with 1.5 mM hydrazine (no buffering, pH 7) at a GC electrode at 50 mV/s. The transverse arrow indicates the start potential and direction of the voltammetric scan.

To further explore the reducing agent of Peak 4, we revisited the voltammetry at a GC electrode in 1.5 mM hydrazine supported by 0.1 M KNO_3 of pH 7, since our previous work [12] reported that the oxidation of $N_2H_5^+$ was electro-inactive at all potentials in the range studied. Fig. 8 shows the voltammetry where a single fully irreversible oxidative peak appears and this peak results (see above) from N_2H_4 oxidation, coincident with our reported observations [12]. No reductive peaks were apparent correlated to the absence of any preceding hydrazinium oxidation. This again is not inconsistent with our above conclusion about Peak 4 (Fig. 3).

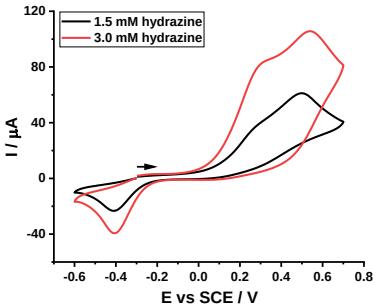

Fig. 9. Voltammograms recorded in 0.1 M KNO_3 with 1.5 mM (black line) and 3.0 mM (red line) hydrazine (no buffering, pH 7) at a Pd electrode at 50 mV/s. The transverse arrow indicates the start potential and direction of the voltammetric scans.

Next a concentration study of hydrazine oxidation at a Pd electrode at pH 7 was performed. The current of the peaks is seen to be rightly doubled when the hydrazine concentration is doubled from 1.5 mM to 3.0 mM as shown in Fig. 9, implying that all

the peaks including peak 4 are hydrazine-related. Note that the direct oxidation of N_2H_4 is, herein, not obvious which is attributed to the very limited concentration of N_2H_4 in the solution of pH 7 (Fig. 1). These experiments further support the idea that Peak 4 is the voltammetrically reductive feature of the $N_2H_5^+$-oxidation product.

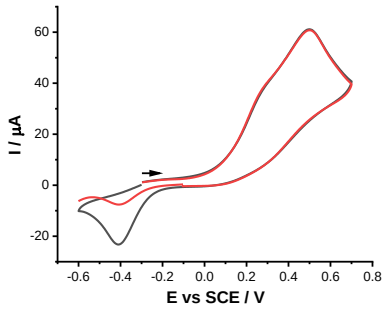

Fig. 10. Voltammograms recorded in 0.1 M KNO_3 with 1.5 mM hydrazine (no buffering, pH 7) at a Pd electrode at 50 mV/s. Black line: a continuous scan; red line: a scan that pauses at -0.1 V for 20 seconds on the back way. The transverse arrow indicates the start potential and direction of the voltammetric scans.

Finally a 'voltammetric stop/start' study was conducted so to affirm the species of the reductant for Peak 4 (Fig. 3). Fig. 10 presents the comparison between a continuous voltammetric scan (black line) and a scan that pauses for 20 seconds at a potential of -0.1 V vs SCE before the reductive scan and the observation of the reduction wave (red line). A marked decrease in the reductive current is discerned after the pause, importantly, indicating the reductant is kinetically unstable on the voltammetric timescale. As is well known that the first electron transfer of hydrazine oxidation is rate-determining [36-40] and the first step involves no protons at the Pd surface [41], hence, it is inferred that the reductant for Peak 4 (Fig. 3) is likely a radical di-cation $N_2H_5^{\bullet 2+}$ from the loss of the first electron of $N_2H_5^+$, which is able to survive for a timescale of seconds. This is also confirmed by the decreasing reductive currents with the rise of pH in Fig. 5 on account of the fact that high hydroxide concentration limits

certainly the formation and probably the lifetime of $N_2H_5^{\bullet 2+}$. Note that studies at lower pH than those reported are precluded since a significant proton reduction on the electrode occurs masking the possible reductive signal of the radical di-cation and leading to the generation of hydrogen gas which distorts the voltammetry.

In the light of the evidence above, we infer that the oxidation of $N_2H_5^+$ very likely forms a radical di-cation $N_2H_5^{\bullet 2+}$ which is stable on the voltammetric timescale (*ca.* seconds). This can be rationalised via the fact that the lone pair on the N adjacent to that being oxidised is pronated and so not available for reaction. We thus further infer that for N_2H_4 the availability of the adjacent lone pair facilitates the rapid reaction following electron transfer. The possible mechanism for hydrazine oxidation at Pd electrodes is proposed as following:

Peak 1: $N_2H_4 \xrightarrow[slow]{-e} N_2H_4^{\bullet +} \xrightarrow[fast]{-3e} N_2 + 4H^+$

Peak 2: $N_2H_5^+ \rightleftharpoons N_2H_4 + H^+$; $N_2H_4 \xrightarrow[slow]{-e} N_2H_4^{\bullet +} \xrightarrow[fast]{-3e} N_2 + 4H^+$

Peak 3: $N_2H_5^+ \xrightarrow{-e} N_2H_5^{\bullet 2+} \xrightarrow{-3e} N_2 + 5H^+$

Peak 4: $N_2H_5^{\bullet 2+} \xrightarrow{+e} N_2H_5^+$

The absence of $N_2H_5^+$ voltammetry on glassy carbon is attributed to the much higher overpotential seen on that material as compared to Palladium. In future work, we will attempt mechanistic modelling and explore the possible roles of surface adsorption and the formation of surface oxides might modulate the mechanism of hydrazine oxidation at diverse catalyst surfaces, especially platinum.

Conclusions

In this work, the mechanism of hydrazine oxidation was studied electrochemically at both Pd and GC electrodes in solutions of different pHs (pH 2, 5, 6, 7, 9.7 and 11). It was found that both the unprotonated hydrazine N_2H_4 and the protonated form $N_2H_5^+$ are *electro-active* at the Pd electrode whereas at the GC electrode only the oxidation of N_2H_4 occurs. Notably, a hitherto unsuspected reductive feature of hydrazine oxidation was observed and clarified as the reduction of a long-lived radical di-cation $N_2H_5^{\bullet 2+}$ which is stable on the voltammetric timescale (*ca.* seconds). Its existence is likely attributed to the fact that the lone pair on the N adjacent to the one being oxidised is pronated and thus not available for reaction, in contrast to N_2H_4 where the available lone pair may facilitate rapid follow up chemical reaction leading to further N-N bonding and the formation of nitrogen, as illustrated in the Fig. 11.

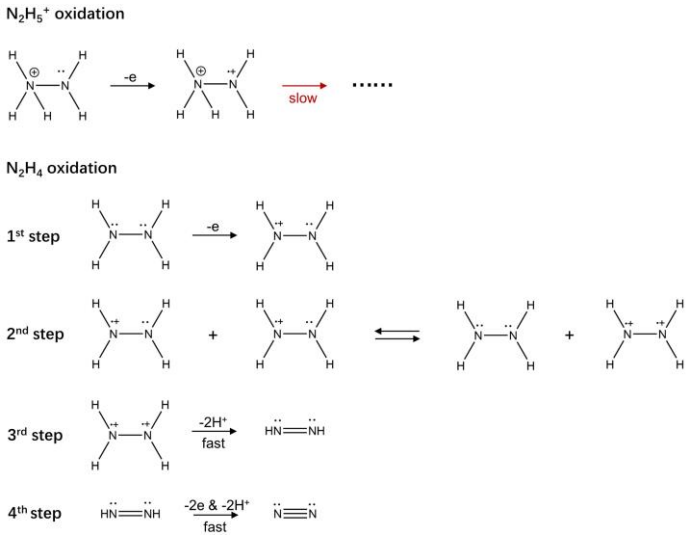

Fig. 11. Schematic diagram for the oxidation of $N_2H_5^+$ and N_2H_4.

Declaration of Competing Interest

The authors declare that they have no known competing financial interests or personal

relationships that could have appeared to influence the work reported in this paper.

Acknowledgements

This paper has been written to mark the occasion of Professor Jens Ulstrup's 80th birthday in recognition of his diverse and deep contributions to electrochemistry.

References

[1] B. Luo, T. Wu, L. Zhang, F. Diao, Y. Zhang, L. Ci, J. Ulstrup, J. Zhang, P. Si, Monometallic nanoporous nickel with high catalytic performance towards hydrazine electro-conversion and its DFT calculations, Electrochim. Acta, 317 (2019) 449-458.
[2] A. Serov, M. Padilla, A.J. Roy, P. Atanassov, T. Sakamoto, K. Asazawa, H. Tanaka, Anode catalysts for direct hydrazine fuel cells: from laboratory test to an electric vehicle, Angew. Chem., 126 (2014) 10504-10507.
[3] H. Wen, G.-X. Cao, M.-H. Chen, Y.-P. Qiu, L.-Y. Gan, P. Wang, Surface phosphorization of hierarchically nanostructured nickel molybdenum oxide derived electrocatalyst for direct hydrazine fuel cell, Appl. Catal. B, 268 (2020) 118388.
[4] Z. Lu, M. Sun, T. Xu, Y. Li, W. Xu, Z. Chang, Y. Ding, X. Sun, L. Jiang, Superaerophobic electrodes for direct hydrazine fuel cells, Adv. Mater., 27 (2015) 2361-2366.
[5] C. Saengsookwaow, R. Rangkupan, O. Chailapakul, N. Rodthongkum, Nitrogen-doped graphene–polyvinylpyrrolidone/gold nanoparticles modified electrode as a novel hydrazine sensor, Sens. Actuators B Chem., 227 (2016) 524-532.
[6] S. Mutyala, J. Mathiyarasu, Preparation of graphene nanoflakes and its application for detection of hydrazine, Sens. Actuators B Chem., 210 (2015) 692-699.
[7] Y. Liu, S.-S. Chen, A.-J. Wang, J.-J. Feng, X. Wu, X. Weng, An ultra-sensitive electrochemical sensor for hydrazine based on AuPd nanorod alloy nanochains, Electrochim. Acta, 195 (2016) 68-76.
[8] M. Zhang, A. Halder, C. Hou, J. Ulstrup, Q. Chi, Free-standing and flexible graphene papers as disposable non-enzymatic electrochemical sensors, Bioelectrochemistry, 109 (2016) 87-94.
[9] L.-S. Wu, X.-P. Wen, H. Wen, H.-B. Dai, P. Wang, Palladium decorated porous nickel having enhanced electrocatalytic performance for hydrazine oxidation, J. Power Sources, 412 (2019) 71-77.
[10] S. Ghasemi, S.R. Hosseini, F. Hasanpoor, S. Nabipour, Amperometric hydrazine sensor based on the use of Pt-Pd nanoparticles placed on reduced graphene oxide nanosheets, Microchim. Acta, 186 (2019) 1-9.
[11] R. Miao, L. Chen, R.G. Compton, Electro-oxidation of hydrazine shows Marcusian electron transfer kinetics, Sci. China Chem., 64 (2021) 322-329.
[12] R. Miao, R.G. Compton, The Electro-Oxidation of Hydrazine: A Self-Inhibiting Reaction, J. Phys.

Chem. Lett., 12 (2021) 1601-1605.
[13] Potassium Phosphate Preparation, AAT Bioquest, Inc, 2021. Retrived from: https://www.aatbio.com/resources/buffer-preparations-and-recipes/potassium-phosphate-ph5-8-to-8-0.
[14] D.R. Lide, CRC Handbook of Chemistry and Physics, CRC press, 2004.
[15] D.L.H. Williams, Nitrosation Reactions and the Chemistry of Nitric Oxide, 1st Elsevier Science, 2004.
[16] A. Radushev, L. Chekanova, V.Y. Gusev, E. Sazonova, Determination of hydrazides and 1, 2-diacylhydrazines of aliphatic carboxylic acids by conductometric titration, J. Anal. Chem., 55 (2000) 445-448.
[17] J.W. Sutherland, Pulse radiolysis of aqueous hydrazine solutions. The triazene species, J. Phys. Chem., 83 (1979) 789-795.
[18] N. Wiberg, Holleman-Wiberg's Inorganic Chemistry, Academic Press, San Diego, 2001.
[19] J.P. Schirmann, P. Bourdauducq, Hydrazine, Ullmann's Encyclopedia of Industrial Chemistry, 2000.
[20] A.Y. Zhakenovich, Y. Valentina, S.T. Tussupbayev Nessipbay, Y. Zhadyra, The Search for New Methods of Synthesis Possible of Organometallic Compounds of P, As, Sb, Bi, J. Chem. Chem. Eng., 9 (2015) 500-502.
[21] J. Zhao, M. Zhu, M. Zheng, Y. Tang, Y. Chen, T. Lu, Electrocatalytic oxidation and detection of hydrazine at carbon nanotube-supported palladium nanoparticles in strong acidic solution conditions, Electrochim. Acta, 56 (2011) 4930-4936.
[22] X. Bo, J. Bai, J. Ju, L. Guo, A sensitive amperometric sensor for hydrazine and hydrogen peroxide based on palladium nanoparticles/onion-like mesoporous carbon vesicle, Anal. Chim. Acta, 675 (2010) 29-35.
[23] R.G. Compton, C.E. Banks, Understanding Voltammetry, World Scientific, Singapore, 2018.
[24] D. Li, C. Lin, C. Batchelor-McAuley, L. Chen, R.G. Compton, Tafel analysis in practice, J. Electroanal. Chem., 826 (2018) 117-124.
[25] B. Wang, X. Cao, The anodic oxidation of hydrazine on glassy carbon electrode, Electroanalysis, 4 (1992) 719-724.
[26] M. Malý, M. Boublík, M. Pocrnić, M. Ansorge, K. Lorinčíková, J. Svobodová, V. Hruška, P. Dubský, B. Gaš, Determination of thermodynamic acidity constants and limiting ionic mobilities of weak electrolytes by capillary electrophoresis using a new free software AnglerFish, Electrophoresis, 41 (2020) 493-501.
[27] J.K. Sa'ib, Titrimetric study of the solubility and dissociation of benzoic acid in water: effect of ionic strength and temperature, Am. J. Chem., 6 (2015) 429.
[28] J. Reijenga, A. Van Hoof, A. Van Loon, B. Teunissen, Development of methods for the determination of pKa values, Anal. Chem. Insights, 8 (2013) ACI. S12304.
[29] Y. Huang, J. Zhang, A. Kongkanand, F.T. Wagner, J.C. Li, J. Jorné, Transient platinum oxide formation and oxygen reduction on carbon-supported platinum and platinum-cobalt alloy electrocatalysts, J. Electrochem. Soc., 161 (2013) F10.
[30] K. Hauff, U. Tuttlies, G. Eigenberger, U. Nieken, Platinum oxide formation and reduction during NO oxidation on a diesel oxidation catalyst–Experimental results, Appl. Catal. B, 123 (2012) 107-116.
[31] V. Rosca, M. Duca, M.T. de Groot, M.T. Koper, Nitrogen cycle electrocatalysis, Chem. Rev., 109

(2009) 2209-2244.
[32] A. Serov, C. Kwak, Direct hydrazine fuel cells: A review, Appl. Catal. B, 98 (2010) 1-9.
[33] M. Petek, S. Bruckenstein, An isotopic labeling investigation of the mechanism of the electrooxidation of hydrazine at platinum: An electrochemical mass spectrometric study, J. Electroanal. Chem. Interf. Electrochem., 47 (1973) 329-333.
[34] F. Cardulla, Hydrazine, J. Chem. Educ., 60 (1983) 505.
[35] L.J. Vieland, R.P. Seward, The Electrical Conductance of Weak Acids in Anhydrous Hydrazine, J. Phys. Chem., 59 (1955) 466-469.
[36] J. Li, X. Lin, Electrocatalytic oxidation of hydrazine and hydroxylamine at gold nanoparticle-polypyrrole nanowire modified glassy carbon electrode, Sens. Actuators B Chem., 126 (2007) 527-535.
[37] M. Shamsipur, Z. Karimi, M.A. Tabrizi, A. Shamsipur, Electrocatalytic Determination of Traces of Hydrazine by a Glassy Carbon Electrode Modified with Palladium - Gold Nanoparticles, Electroanalysis, 26 (2014) 1994-2001.
[38] P.K. Rastogi, V. Ganesan, Krishnamoorthi, Palladium nanoparticles decorated gaur gum based hybrid material for electrocatalytic hydrazine determination, Electrochim. Acta, 125 (2014) 593-600.
[39] B. Alvarez-Ruiz, R. Gomez, J. Orts, J. Feliu, Role of the metal and surface structure in the electro-oxidation of hydrazine in acidic media, J. Electrochem. Soc., 149 (2002) D35.
[40] H. Hamidi, S. Bozorgzadeh, B. Haghighi, Amperometric hydrazine sensor using a glassy carbon electrode modified with gold nanoparticle-decorated multiwalled carbon nanotubes, Mikrochim Acta, 184 (2017) 4537-4543.
[41] R. Miao, L. Shao, R.G. Compton, Single entity electrochemistry and the electron transfer kinetics of hydrazine oxidation, Nano Res., (2021).